SUPPORTING INFORMATION

Integrated MicroHall Magnetometer to Measure Magnetic Properties of Nanoparticles

Changwook Min[1,7], Jongmin Park[1], Jae Kyoung Mun[2], Yongjun Lim[3,4,5], Jouha Min[1], Jong-Won Lim[2], Dong-Min Kang[2], Ho-Kyun Ahn[2], Tae-Hyun Shin[3,4,5], Jinwoo Cheon[3,4,5], Hae-Seung Lee[6], Ralph Weissleder[1,8], Cesar M. Castro[1], Hakho Lee[1,3,4]

1. Center for Systems Biology, Massachusetts General Hospital, Harvard Medical School, Boston, MA 02114
2. ICT Materials & Components Research Laboratory, ETRI, Daejeon 34129, Republic of Korea
3. Center for NanoMedicine, Institute for Basic Science (IBS), Seoul 03722, Republic of Korea
4. Yonsei-IBS Institute, Yonsei University, Seoul 03722, Republic of Korea
5. Department of Chemistry, Yonsei University, Seoul 03722, Republic of Korea
6. Department of Electrical Engineering, MIT, Cambridge, MA 02139
7. Harvard-MIT Division of Health Sciences and Technology, MIT, Cambridge, MA 02139
8. Department of Systems Biology, Harvard Medical School, Boston, MA 02115

SUPPLEMENTARY FIGURE

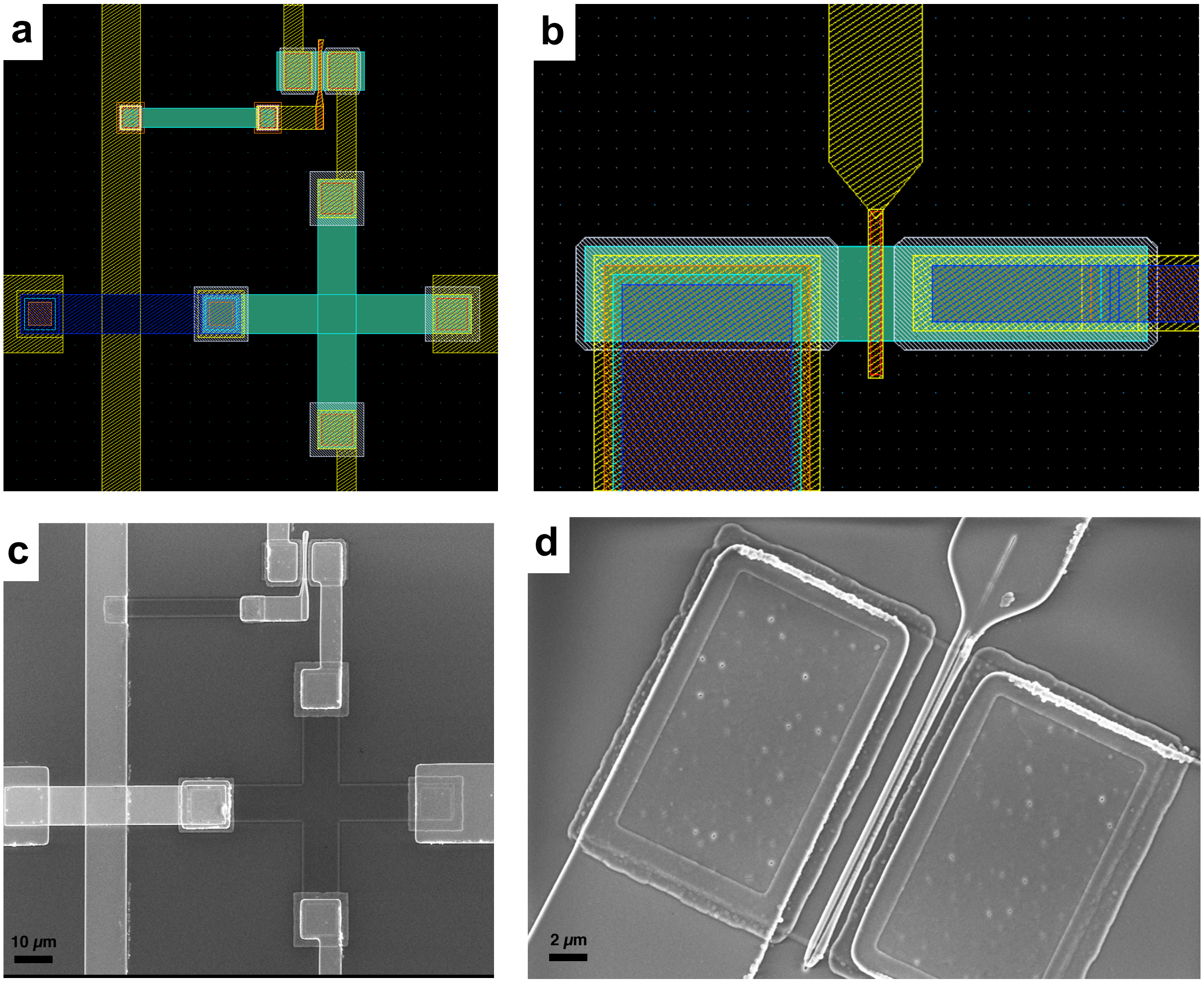

Figure S1. CAD Layout and SEM Images of μHall chip. (a) Layout of μHall element and transistor switch. **(b)** Layout of PHEMPT (pseudomorphic high electron mobility transistor) amplifier with single finger. **(c)** SEM Image of μHall element and transistor switch. **(d)** SEM Image of PHEMPT amplifier with single finger.

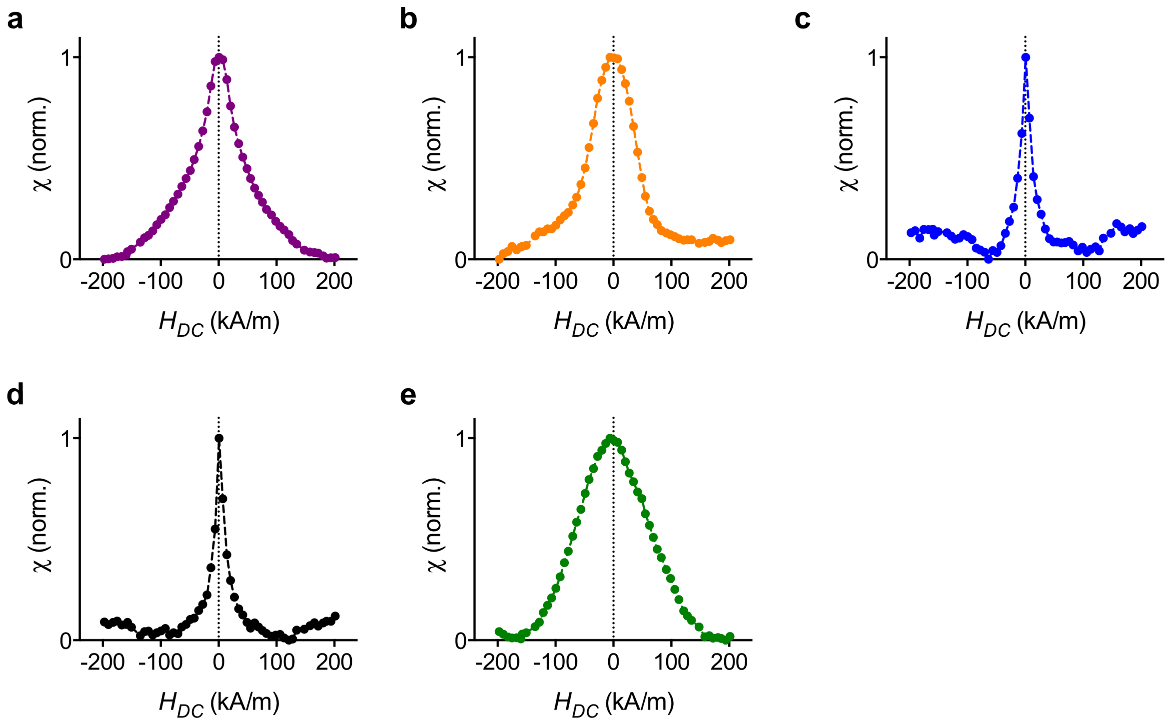

Figure S2. Multichannel measurement of MNPs. Magnetic susceptibility curves of various types of MNPs were measured in different channels of the microHall array: $Zn_{0.6}Fe_{2.6}O_4$ (a), Spherotech SVM-025-5H (b), Dynabead MyOne 65602 (c), Dynabead M-280 11205D (d), $CoFe_2O_4$ (e).

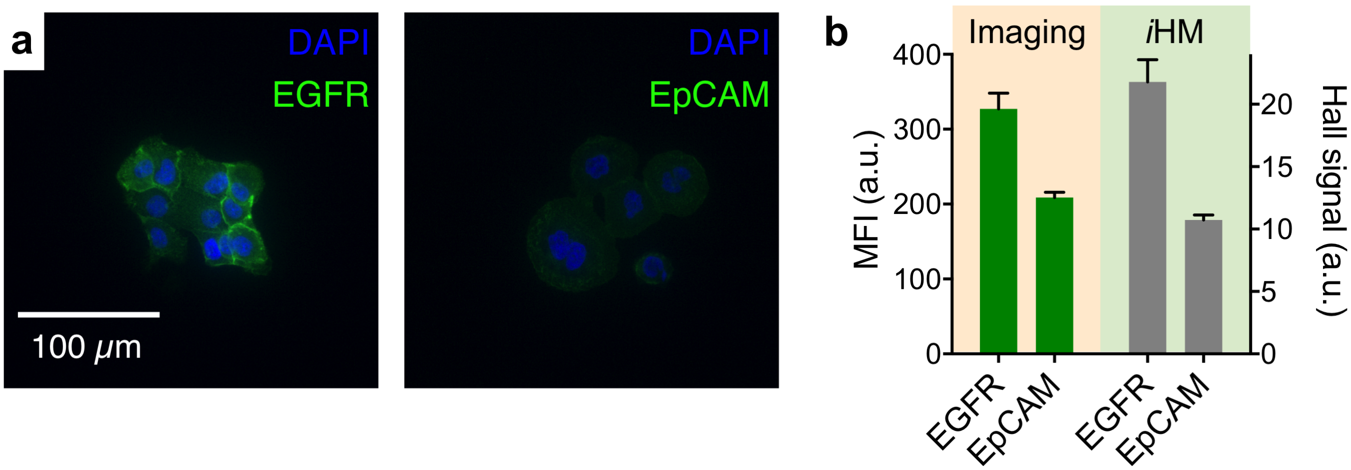

Figure S3. Immunofluorescence microscopy of OVCA420. (a) OVCA420 cells were labeled with fluorescent antibodies and imaged. Fluorescent intensity from EGFR immunostaining (left) was higher than that from EpCAM staining. **(b)** Quantification of molecular expression levels in OVCA420. Mean fluorescence intensity (MFI) was calculated for EGFR and EpCAM expressions. The profiling results from imaging agreed well the *i*HM data.

SUPPLEMENTARY NOTE

Symbols used in the text

	Description		Description
V_H	Hall voltage (Hall element)	T	Temperature
$V_{H.Lock}$	Hall voltage (from lock-in amplifier)	ω_0	frequency of time varying magnetic field
B	total magnetic induction	n	number density
H	magnetic field strength	V	volume
M	magnetization of material	G	magneto-geometrical factor
H_{DC}	external magnetic field (static)	R_H	Hall coefficient
H_{AC}	external magnetic field (time varying)	t	thickness of device
μ_p	magnetic moment	I	DC bias current
χ_V	magnetic susceptibility	μ_0	vacuum permeability
χ_0	magnetic susceptibility at H=0	k_B	Boltzmann constant

1. Hall output is proportional to magnetic susceptibility at the given DC polarization field.

Hall voltage, V_H, is given by[1,2]

(1) $$V_H = \frac{GR_H}{t} IB$$

If external magnetic fields, H_{DC} and H_{AC}, are applied perpendicular to Hall sensor plane, then magnetic field induction, B, is sum of external magnetic field strength and induced magnetic field from magnetic materials.

(2) $$B = \mu_0 \left[H_{DC} + H_{AC} e^{jw_0 t} + M(H) \Big|_{H = H_{DC} + H_{AC} e^{jw_0 t}} \right]$$

where

(3) $$B = \mu_0 (H + M(H))$$

(4) $$H = H_{DC} + H_{AC} e^{jw_0 t}$$

Using Eq. (2), V_H is expressed as

(5) $$V_H = \frac{\mu_0 G R_H}{t} I \bullet \left[H_{DC} + H_{AC} e^{jw_0 t} + M(H_{DC} + H_{AC} e^{jw_0 t}) \right]$$

The first order of Taylor approximation of Eq. (5) leads to

(6) $$V_H \simeq \frac{\mu_0 G R_H}{t} I \bullet \left(H_{DC} + H_{AC} e^{jw_0 t} + M(H_{DC}) + \frac{dM}{dH}\Big|_{H=H_{DC}} \bullet H_{AC} e^{jw_0 t} \right)$$

Frequency modulated Hall voltage is down-converted to DC signal by lock-in amplifier. Then Eq. (6) can be written as a function of magnetic susceptibility.

(7) $$\begin{aligned} V_{H.Lock} &= \frac{\mu_0 G R_H}{t} I \bullet \left(H_{AC} + \frac{dM}{dH}\Big|_{H=H_{DC}} \bullet H_{AC} \right) \\ &= \frac{\mu_0 G R_H}{t} I H_{AC} \bullet \left(1 + \frac{dM}{dH}\Big|_{H=H_{DC}} \right) \\ &= \frac{\mu_0 G R_H}{t} I H_{AC} \bullet \left[1 + \chi_V (H_{DC}) \right] \end{aligned}$$

2. Normalized magnetic susceptibility

Magnetization of superparamagnetic nanoparticles is given as[3,4]

(8) $$M(H) = M_0 \cdot \left[\coth\left(\frac{\mu_0 \mu_p H}{k_B T} \right) - \left(\frac{k_B T}{\mu_0 \mu_p H} \right) \right]$$

where

(9) $$M = \frac{m}{V}$$

$$M_0 = n\mu_p \tag{10}$$

From Eq. (8), we can obtain magnetic susceptibility by differentiating magnetization with respect to magnetic field strength.

$$\begin{aligned} \frac{dM}{dH} &= M_0 \cdot \frac{\mu_0\mu_p}{k_B T} \cdot \left[-\csc h^2\left(\frac{\mu_0\mu_p H}{k_B T}\right) + \left(\frac{\mu_0\mu_p H}{k_B T}\right)^{-2} \right] \\ &= M_0 \cdot \frac{\mu_0\mu_p}{3k_B T} \cdot 3 \cdot \left[-\csc h^2\left(\frac{\mu_0\mu_p H}{k_B T}\right) + \left(\frac{\mu_0\mu_p H}{k_B T}\right)^{-2} \right] \\ &= \chi_0 \cdot 3 \cdot \left[-\csc h^2\left(\frac{\mu_0\mu_p H}{k_B T}\right) + \left(\frac{\mu_0\mu_p H}{k_B T}\right)^{-2} \right] \end{aligned} \tag{11}$$

Therefore, normalized magnetic susceptibility becomes

$$\frac{\chi_v}{\chi_0} = 3 \cdot \left[-\csc h^2\left(\frac{\mu_0\mu_p H}{k_B T}\right) + \left(\frac{\mu_0\mu_p H}{k_B T}\right)^{-2} \right] \tag{12}$$

3. Effect of Hall sensor geometry

Geometry of Hall element affects Hall voltage output as described in Eq. (1). We could further evaluate the effect of Hall sensor geometry by analyzing signal to thermal noise ratio. The magnetic field resolution ($T / \sqrt{Hz}$) is given as[2]

$$B_{\min} \equiv \frac{\sqrt{4kTR}}{V_H / B} = \frac{\sqrt{4kTR}}{S_I I} = \frac{\sqrt{4kTM}}{v\sqrt{\mu en} G(w/l)\sqrt{wtl}} \tag{13}$$

As shown in Eq. (13), the minimum magnetic field that the Hall sensor could detect is a function of width (w), length (l), and thickness (t) of the Hall sensor cross.

4. Hall voltage and sample position

The magnetic induction at the position **r** from the Hall sensor surface is given as[4]

(14) $$\vec{B}(\vec{r}) = \mu_0 \overrightarrow{H_e} + \frac{\mu_0}{4\pi} \cdot \frac{3(\vec{r} \cdot \overrightarrow{MV})r - (\vec{r} \cdot \vec{r})MV}{r^5}$$

where

(15) $$H_e = H_{DC} + H_{AC} e^{jw_0 t}$$

(16) $$M(H) \approx M(H_{DC}) + \frac{dM}{dH}\Big|_{H=H_{DC}} \bullet H_{AC} e^{jw_0 t}$$

After plugging Eq.(14) into Eq.(1), V_H is a function of the sample position **r**. And V_H is inversely proportional to r^3 if the directions of induced magnetization and position vector are in parallel.

5. Size of sample chamber

Effective sensing volume of the Hall sensor determines the size of microfluidic chamber. Based on our sensitivity measurement, the minimum magnetic field (B_{min}) that the Hall element can detect is B_{min} = 0.15 µT, which is equivalent to 0.1 µV in the Hall voltage output ($V_{H.Lock}$) from lock-in measurement with 2 sec integration time. We assume that a magnetic particle (diameter d = 1 µm, saturation magnetization M = 336 kA/m)[5] is positioned above the Hall sensor. The field from the bead can be approximated as

(17) $$B = \frac{\mu_0}{4\pi} \cdot \frac{2}{r^3} \cdot \left(\frac{4\pi}{3} \cdot \frac{d^3}{8} \cdot M \right).$$

Setting $B > B_{\min}$, we get $r < 6$ µm. The maximum distance within which the particle can still be detected is ~ 6 µm. Therefore the effective sensing volume of the Hall sensor (l = 7 µm, w = 7 µm) will be 19 µm (l) × 19 µm (w) × 6 µm (h). If the size of the chamber is larger than the effective sensing volume, the Hall sensor output could not detect the signal from the area beyond the effective sensing volume. We chose the size of the microfluidic chamber based on the effective sensing volume and the size of single cancer cell.

REFERENCE

1. Popovic, R. S. Hall Effect Sensors. Institute of Physics Publishing Bristol and Philadelphia, Bodmin, Cornwall (2004).
2. Boero, G., Demierre, M., Popovic, R. S. & others. Micro-Hall devices: performance, technologies and applications. *Sensors and Actuators A: Physical* **106**, 314-320 (2003).
3. Rado, G. Magnetism V1, Volume 1. *Elsevier Science* (1963).
4. Besse, P.-A., Boero, G., Demierre, M., Pott, V. & Popovic, R. Detection of a single magnetic microbead using a miniaturized silicon Hall sensor. *Applied Physics Letters* **80**, 4199-4201 (2002).
5. Fonnum, G., Johansson, C., Molteberg, A., Mørup, S., Aksnes, A. Characterisation of Dynabeads by magnetization measurements and Mossbauer spectroscopy. *Journal of Magnetism and Magnetic Material*s **293,** 41–47 (2005).